

Rotation Effects on a Horizontal Axis Wind Turbine Blade

Mohamed Mehdi Oueslati^{#1}, Anouar Wajdi Dahmouni^{#2}, Sassi Ben Nasrallah^{*3}

[#] *Laboratory of Wind Energy Management and Waste Energy Recovery, Research and Technologies Center of Energy Ecoparck of Borj-Cedria, BP 95 Hammam lif 2050, Tunisia.*

¹mehdi.oueslati@crten.rnrt.tn

²dahmouni_anouar_wajdi@yahoo.fr

^{*}*Laboratory of Thermal and Energy Systems Studies*

National Engineering School of Monastir, Street Ibn El Jazzar, Monastir 5000, Tunisia

³sassi.bennasrallah@enim.rnu.tn

Abstract— The wind turbine blades are influenced by many physical phenomena caused by the unsteady environment conditions and the rotation effects. In this context, a three-dimensional simulations of the flow around a horizontal axis wind turbine model was performed with the Fluent 6.3.26 software to study the performances of the rotating blades. The k- ϵ turbulence model and the Moving Reference Frame (MRF) technique, have been used to taken into account the flow turbulence and the rotating effects respectively. The analysis of the flow separation over the blades has been examined under different tip speed ratios of the wind turbine for a constant wind speed value. The obtained results show that the angular velocity of the rotor affects the flow separation behavior, the streamlines, and the pressure distribution over the blade.

Keywords— Horizontal axis wind turbine, Rotating blade, Three-dimensional simulations, k- ϵ turbulence model.

I. INTRODUCTION

To evaluate wind turbine performances it's necessary to examine the flow over the rotor, and take into account the different physical phenomena that can be present during the system operation.

Due to the expensive cost of the experiments and the difficulties to control the different physical parameters, many researchers were used the fully three-dimensional simulations in complete geometry of wind turbines despite the high time of computing and the need for large capacity calculating machines.

Johansen *et al.* [1] have developed a CFD solver, EllipSys3D, with a stationary RANS model to evaluate the three-dimensional aerodynamic coefficients in different radial positions along the blade. The obtained results were injected into a Blade Element Momentum (BEM) code without additional corrections. They showed excellent compatibility with experimental results for cases when the flow is attached and when small separation flow occurs.

Chaviaropoulos *et al.* [2] have solved the Navier Stokes equations in three-dimensional formulation to determine the aerodynamic coefficients under three-dimensional effects.

They have remarked that the lift and drag coefficients increase compared with the two-dimensional coefficients and they can be expressed in terms of the chord length, the radius of the rotor and of the local angle of attack.

Carangiu *et al.* [3] have developed a three-dimensional CFD model to analyze the influence of the radial flow on the performances of a horizontal axis wind turbine in the range of Reynolds numbers greater than 10^6 . They have examined the behavior of the boundary layer over the wind turbine blades and they confirmed the increase of the aerodynamic coefficients, however, their results have not been validated experimentally.

Shen *et al.* [4] have developed an analytical method to determine the relative angle of attack of the airfoil and its aerodynamic coefficients at each blade section along horizontal axis wind turbine blade using a three-dimensional CFD simulations. The simulations were carried out in full geometry case of "Tellus" wind turbine which has 95 kW of power using the EllipSys3D solver with a fully turbulent RANS model. By assuming that the transition effects are very limited in the case of the large rotor, they have confirmed the existence of the dynamic stall phenomenon which increase the forces acting on the rotor blades.

Yu *et al.* [5] have performed three-dimensional CFD calculations using RANS equations and k- ω SST turbulence model of the NREL horizontal axis wind turbine Phase VI, operating under transition flow conditions. They showed a good agreement with the existent experimental results for wind speed lower than 10 m/s. Under these conditions, they extrapolated the lift and drag coefficients at angles of attack up to 20° .

Herráez *et al.* [6] have recently modeled the rotor of the horizontal axis wind turbine of the MEXICO project using the three-dimensional CFD solver, OpenFoam, coupled with the single-Spalart Allmaras turbulence model. Their model has been validated by plotting the distribution of the pressure coefficient C_p in comparison with experimental results obtained by PIV measurements. They have confirmed the presence of the dynamic stall phenomenon and the increase of

the lift coefficient due to the rotation of the blade. They have attributed the phenomenon of the dynamic stall to the Coriolis force and the increase of the lift coefficient to the centrifugal force.

Since the studies of the flow characteristics on a rotating wind turbine blades are limited, in this paper three-dimensional simulations of the flow over a horizontal axis wind turbine model have been performed using the Fluent software and the k-ε turbulence model, to study the influence of the physical parameters and the tip speed ratio on the blade performances.

II. NUMERICAL APPROACH AND RESULTS

The horizontal axis wind turbine model used during the simulations is a three-bladed rotor with 376 mm of diameter. As shown in Figure 1, the model has a hub diameter equal to 60 mm and a nacelle length of 205 mm.

The blades are built based on the NACA 4412 airfoil (Fig. 2) and characterized by a length of 150mm, a constant chord, c, equal to 50 mm and a fixed pitch angle equal to 14.5°.

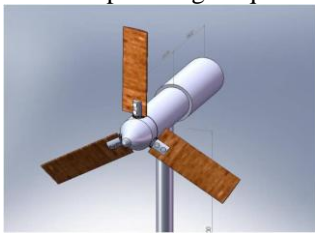


Fig. 1 Three dimensional horizontal axis wind turbine model

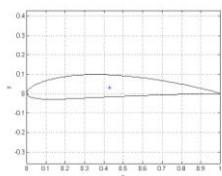


Fig. 2 NACA 4412 airfoil

A. Grid Generation

The GAMBIT software was used to build the mesh around the wind turbine model described above. The geometry of the considered configuration is shown in Figure 3. The wind turbine was placed in a rectangular channel with the same dimensions of the wind tunnel of the Research and Technology centre of Energy (CRTE).

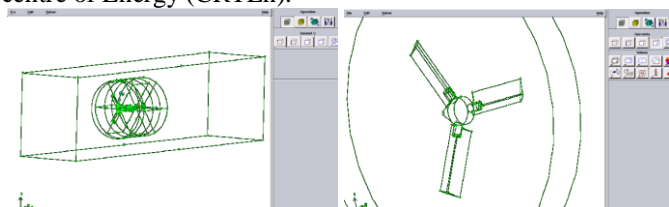


Fig. 3 Gambit geometry configuration

The domain was divided into three regions: the external flow of the channel, the flow around the rotor and the region behind the rotor where the near wake will be explored. The structure of the mesh differs from one region to another. It was

a non structured tetrahedral grid around the rotor and into the channel while it was structured hexahedral grid in the near wake of the wind turbine.

The total mesh consists of 3,324,776 cells. The mesh refinement was focused in the near wake downstream of the wind turbine, at the positions of the tip and root vortices and around the blades in the radial direction. The Figure 4 shows the grid refinement downstream of the wind turbine.

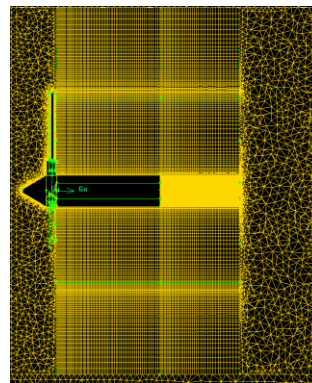


Fig. 4 Grid at the near wake region behind the wind turbine

B. Boundary conditions

The computational domain and the boundary conditions used are shown in Figure 5. In fact, the wind turbine was placed in a rectangular channel with $1000 \times 800 \text{ mm}^2$ section which is the same size of the wind tunnel of the CRTE. The computational domain was divided into three main parts.

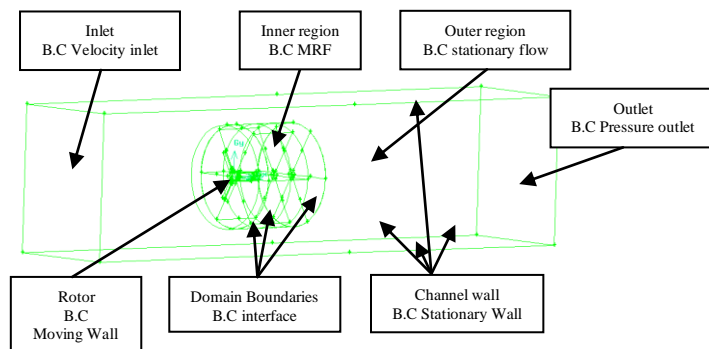


Fig. 5 Boundary conditions

The first region corresponds to the geometry of the channel which has a total length equal to 4000 mm corresponding to a distance equal to $21 \times R$ (where R is the radius of the wind turbine model). The input and output boundary conditions of the channel as well as the fixed walls were designated as "velocity inlet", "pressure outlet" and "stationary wall" respectively.

The Figure 6 illustrates the second region including the rotor of the wind turbine.

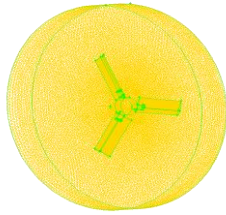


Fig. 6 Grid in the domain around the rotor

The boundary conditions associated to the rotor was "Moving Wall" and the flow field around the rotor as a "Moving Reference Frame (MRF)".

As the second region, the fluid domain of the third region presented in figure 7 was associated to "Moving Reference Frame", and the wind turbine nacelle was associated to "Stationary Wall" and the domain boundaries were intended as "interface".

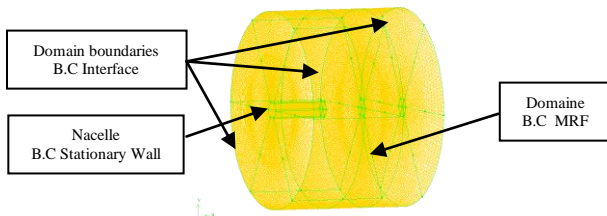


Fig. 7 Grid and boundary conditions of the region behind the wind turbine

The mobile reference system technique in Fluent (MRF: Moving Reference Frame) was used in the simulations to model the moving parts by the activation of the mobile referential systems in the selected area. When this option is enabled, the equations of motion are modified to incorporate the terms of Coriolis acceleration.

The k-ε Standard turbulence model was used during the simulations. The table below summarizes the conditions of simulations used under Fluent software.

TABLE I
FLUENT CONDITIONS OF SIMULATION

Simulation type	3D unsteady
Type of flow	Incompressible
Algorithme CFD	Simple
Modèle de turbulence	k-ε Standard
Schéma d'interpolation	Pression Standard Densité Second Ordre Moment Second ordre Upwind Viscosité turbulente Second ordre
Nombre de Nœuds	3 324 776

C. Results and Discussions

Figure 8 illustrates the axial velocity iso-surfaces in the near wake of the wind turbine obtained from the CFD calculations. It is observed that the near wake downstream is characterized by the detachment of the tip and root vortices from the blades. The helical nature of the vortex shedding is also observed.

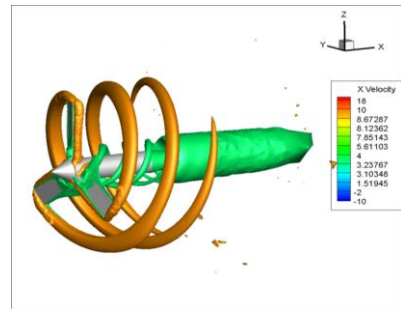


Fig. 8 Three dimensional axial velocity iso-surfaces

The rotation of the turbine blades causes the creation of a separation zone under the effect of the centrifugal force. Figure 9 illustrates the three-dimensional streamlines of the flow downstream the rotor blade and shows the flow separation from its the suction side in the radial direction.

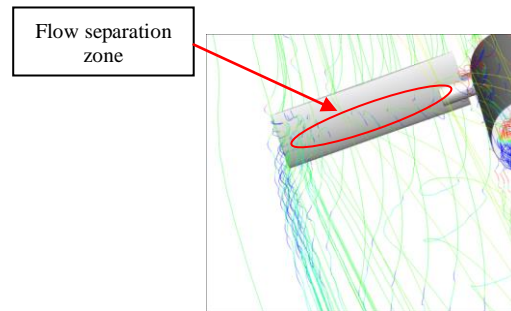


Fig. 9 Three dimensional streamlines behind the rotor blade

To study the effect of the tip speed ratio on the flow separation features, the streamlines on the pressure side and the suction side of the wind turbine blades have been presented in Figures 10 and 11 respectively for five different tip speed ratios $\lambda = 2.48, 3.41, 4.08, 4.65$ and 6.2 .

Figure 10 shows the flow separation about 37% of the pressure side blade then it reattaches at 60% for lower value of tip speed ratio $\lambda = 2.48$. The separation zone decreases as the tip speed ratio increases and the flow becomes fully attached to the blade surface as observed in the case of $\lambda = 4.65$ and $\lambda = 6.2$.

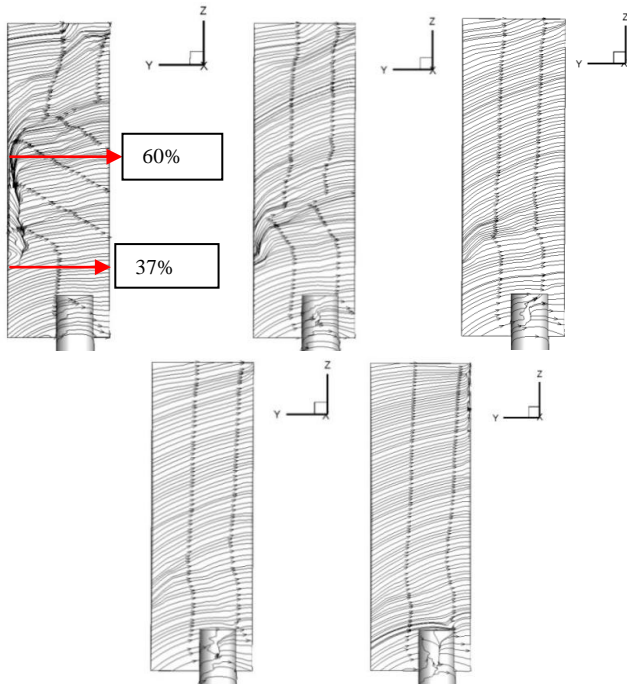


Fig. 10 Streamlines at the pressure side of the blade for different tip speed ratio

On the suction side of the wind turbine blade (the Fig.11), the flow separation region occurs close to the leading edge and decreases with increasing the tip speed ratio λ . For high values of λ , the separation line is located at a distance equal to 1/3 of the chord length from the leading edge.

We can conclude that the flow separation at different sections of the blade is influenced by the tip speed ratio of the wind turbine. This is due to the increase of the centrifugal force which affects the pressure distribution on the blade surfaces

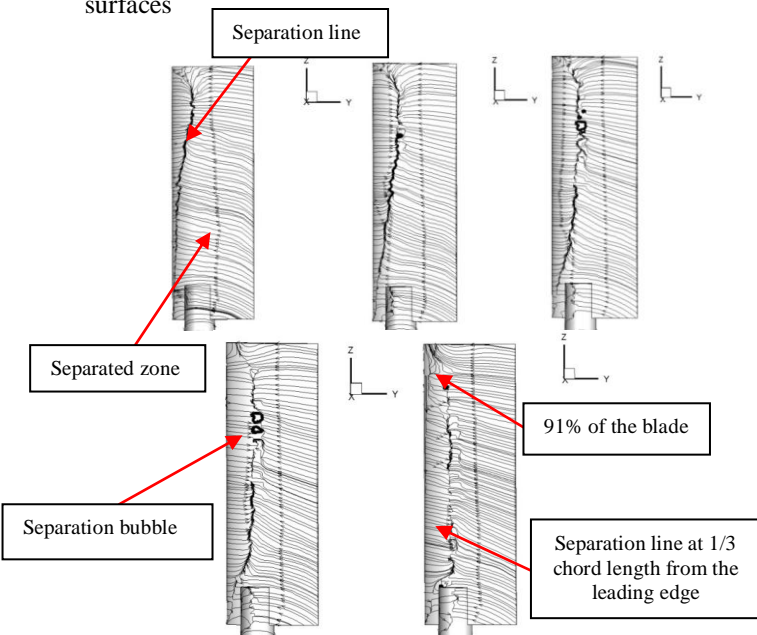


Fig. 11 Streamlines at the suction side of the blade for different tip speed ratio

To evaluate the effects of the centrifugal force on the aerodynamic performances of the blade, the Figure 12 shows the distribution of the static pressure on the suction side of the blade for different tip speed ratios of the wind turbine as $\lambda = 2.48, 3.41, 4.08, 4.65$ and 6.2 respectively.

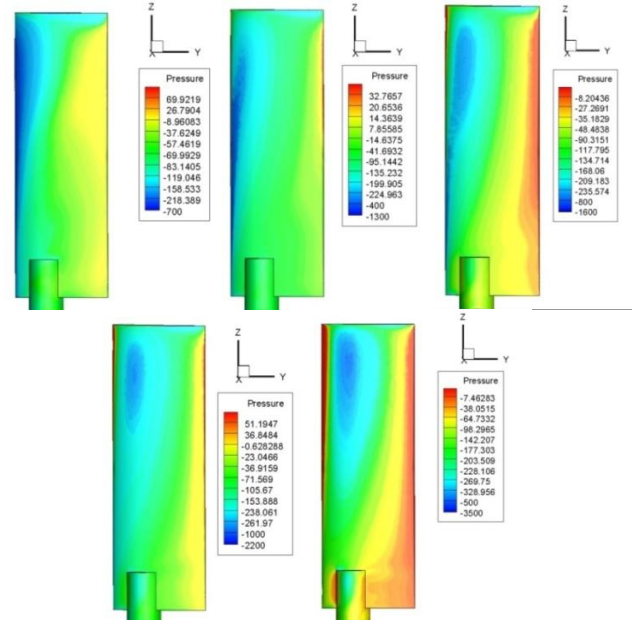


Fig. 12 Static pressure distribution at the suction side of the blade for different tip speed ratio.

It is noted that the centrifugal force causes the creation of a negative pressure zone along the blade at the leading edge. By increasing the tip speed ratio of the wind turbine, the depression region increases in the radial direction and deflects its orientation. The maximum value of the depression zone is located near the upper end of the blade. This affects the pressure coefficient distribution at each blade section depending on the tip speed ratio.

To analyze this behavior, the pressure coefficient distribution at different section location of the blade was calculated using the following equation:

$$C_p = \frac{P - P_\infty}{1/2\rho[(V_R - \omega r)^2 + U_R^2]}$$

Figure 13 shows the pressure coefficient distribution at different sections of the blade $r/R=0.5, 0.7$ and 0.9 for $\lambda = 4.08$.

We can remark that the pressure coefficient vary along the blade. This is due to the variation of the angle of attack at each blade section and the flow separation characteristics in the radial direction.

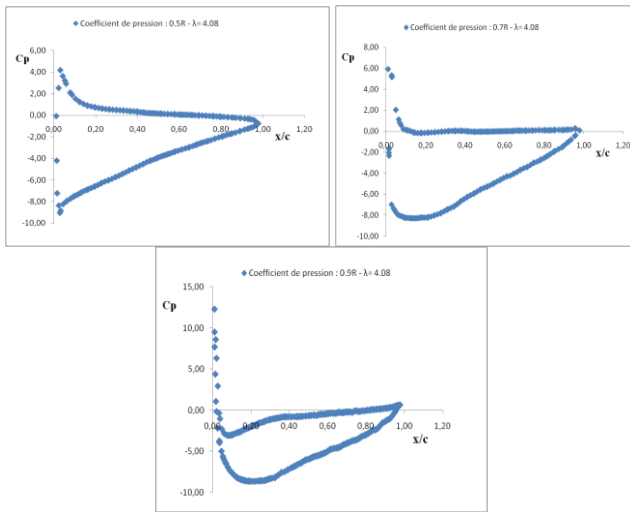


Fig. 13 Pressure coefficient distribution at different blade section $r/R=0.5$, 0.7 , 0.9 and tip speed ratio 4.08

To study the effect of the tip speed ratio on the pressure coefficient distribution, Figure 14 shows the evolution of the pressure coefficient on each section of the blade for tip speed ratio equal to 3.42 , 4.08 and 4.65 .

The C_p curves show that the pressure coefficient decreases near the leading edge when the wind turbine rotation speed increases.

Indeed, for the position $r/R = 0.5$, a slight decrease of the pressure coefficient was observed since the flow is still attached to the blade in this region.

By approaching to the upper end of the blade in the radial positions $r/R = 0.7$ and 0.9 , there is a significant decrease of the pressure coefficient at the leading edge. In addition, there is a gradual increase in the maximum pressure coefficient value while approaching to the upper end of the blade. The decrease of the pressure coefficient increases the aerodynamic forces on the wind turbine blades.

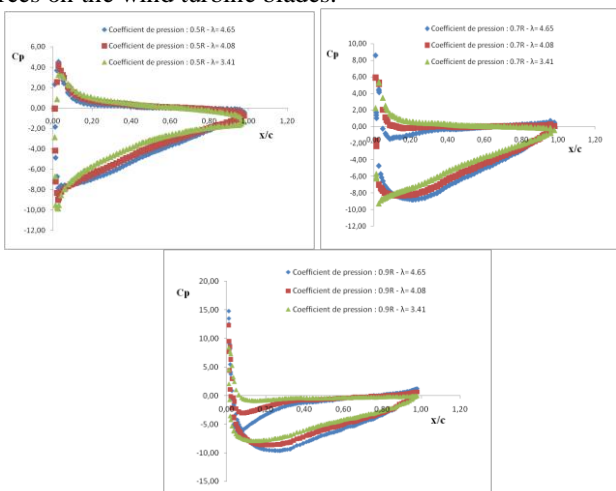


Fig. 14 Pressure coefficient distribution at different blade section for different tip speed ratio 3.42 , 4.08 and 4.65

III. CONCLUSIONS

In this paper a numerical analysis of the performances of a horizontal axis wind turbine has been performed. Three-dimensional simulations coupled by the $k-\epsilon$ turbulence model using the Fluent software has been investigated.

The flow separation characteristics at the pressure side and the suction side of the three dimensional blade has been studied in function of the tip speed ratio. The results show that the centrifugal force affects the performances of the blade by the decrease of the pressure coefficient at the leading edge at each blade section in the radial direction.

REFERENCES

- [1] J. Johansen, N. N. Sørensen, "Aerofoil Characteristics from 3D CFD Rotor Computations," *Wind Energy*, vol. 7, pp. 283–294, 2004.
- [2] P. K. Chaviaropoulos, M. O. L. Hansen, "Investigating Three-Dimensional and Rotational Effects on Wind Turbine Blades by Means of a Quasi-3D Navier Stokes Solver," *J. Fluids Engineering*, vol. 122, pp 330–336, 2000.
- [3] C. E. Carcangiu, J. N. Sørensen, F. Cambuli, N. Mandas, "CFD–RANS analysis of the rotational effects on the boundary layer of wind turbine blades," *Journal of Physics: Conference Series*, vol. 75, 2007.
- [4] W. Z. Shen, M. O. L. Hansen and J. N. Sørensen, "Determination of the Angle of Attack on Rotor Blades," *Wind Energy*, Vol. 12, pp 91–98, 2009.
- [5] G. Yu, X. Shen, X. Zhu, Z. Du, "An insight into the separate flow and stall delay for HAWT," *Renewable Energy*, vol. 36, pp 69–76, 2011.
- [6] I. Herráez, B. Stoevesandt, J. Peinke, "Insight into Rotational Effects on a Wind Turbine Blade Using Navier–Stokes Computations," *Energies*, vol. 7, pp 6798–6822, 2014.